Experimental Validation of a Model-Free Controller on a One-Axis Float with Ballast

Loïck Degorre, Gabriel Betton, Emmanuel Delaleau, Riera Mathis, Luc Jaulin, Lionel Lapierre

Preprint - Experimental Validation of a Model-Free Controller on a One-Axis Float with Ballast

Loïck Degorre*, Gabriel Betton*, Emmanuel Delaleau**, Mathis Riera***, Luc Jaulin* and Lionel Lapierre* ‡

March 18, 2025

Abstract

A large proportion of underwater vehicles use a ballast or a bladder for depth control. This is notably the case for most gliders and a variety of drifters, buoys, and floats used in oceanography, marine biology, etc. Their regulation in depth usually requires good knowledge of their model and is subject to external disturbances. This work presents the application of Model-Free Control (MFC) to a one-axis float equipped only with a ballast and a depth sensor. MFC is well-suited for this application as it is completely model-oblivious and particularly robust to external disturbances. The two main contributions of this work are the first development of a third-order model-free controller and the experimental validation of the method on a fairly simple system with minimum actuation, the float with ballast. The main objective of this work is to put MFC on the map of control methods suited for marine applications and introduce this method to the community with a rather simple yet striking example.

1 Introduction

This work presents the first application of the Model-Free Control (MFC) approach to a diving float equipped only with a ballast and a depth sensor. The float with ballast represents the simplest and most broadly spread underwater systems. Applications like marine life monitoring, oceanography, sample picking, drifting measures at constant depth, or inspection programs make use of

** Loïck Degorre, Gabriel Betton, Luc Jaulin and Lionel Lapierre are with ENSTA, UMR 6285, IPP Lab-STICC, F-29 200 Brest, France. Contact e-mail: loick.degorre@ensta.fr

†** Emmanuel Delaleau is with ENI Brest, UMR CNRS 6027, IRDL, F-29 200 Brest, France.

‡*** Mathis Riera is with Université de Toulon, COSMER - EA 7398 CS 60584, 83041 Toulon CEDEX 9, France.

one float, a fleet of floats, or underwater vehicles equipped with ballasts e.g. the *Argo* program [1]. Also, gliders represent the majority of Autonomous Underwater Vehicles (AUV) and are often equipped with ballasts or bladders used for depth actuation as well as of its forward motion through hydrodynamic couplings.

This work proposes a new solution for depth regulation of a float system equipped only with a ballast and an entry-level depth sensor without knowledge of the model of the craft and on several trajectories of increasing complexity. The robustness of the controller to external disturbances is experimentally assessed. The aim of this study is to show a new application of MFC and put the method on the map of control methods suited for the marine environment.

Related Works

A review of the most common actuation technologies of float systems can be found in [2]. Ballasts are used in simple float systems and underwater vehicles to control the weight-to-buoyancy ratio of the craft. They represent a minimalistic and energy-efficient solution, particularly interesting for long-range and long-term missions. Yet, in most applications, ballasts are used as safety systems or in an all-or-nothing fashion for very simple depth control. Several technologies coexist for various applications. For the deepest waters, the ballast is composed of a flexible compartment filled with oil [3]. For shallower depths, as in this work, the ballast is composed of a simple plunger, often actuated with a DC motor and a screw-gear system, filling with water [4] or modifying the submerged volume of the craft [5].

In terms of control, standard PID controllers do not perform satisfactory in stabilizing the depth of a vehicle equipped with a ballast. The system is non-linear and can be subject to severe disturbances. The work of [2] proposes a segmented PD controller switching between speed and depth regulation. Feedback Linearization methods are often preferred [4]. Yet, they require good knowledge or precise estimation of the model of the vehicle, which can prove cumbersome. For increased robustness to model approximations, [6] proposes a LQR controller which, when compared to standard two-stage PDs, behaves well. Other approaches like Sliding-Mode Control (SMC) can be found [7]. Yet, even though the robustness of SMC is particularly beneficial for marine applications, it comes with well-known constraints like chattering and a relatively high energy expenditure at and around equilibria that are not acceptable for ballast-actuated depth regulation. The conventional constraints of these methods are overcome with Fuzzy control in [8] or with Active Disturbance Rejection Control (ADRC) [9].

In this work, a model-oblivious, yet very robust method is preferred: Model-Free Control (MFC). MFC was introduced in 2006 in France [10]. One refers to [11] which is a review and a detailed exposition and, more recently [12]. Many applications of this approach have been developed since then and are too numerous to be all cited here. One notable example though is the application of MFC to the quadrotor drone [13]. However, to the authors' best knowledge, only

one application of MFC in the marine environment exists as of today; the work of [14] where iPDs are used to regulate the forward motion of an overactuated AUV.

This work is also the first example where a third order model-free controller appears mandatory. This goes against the original claims of MFC where orders 1 or 2 were supposed to be sufficient to cover most if not all physical-based model [11]. As is demonstrated in the following, the float with ballast must be controlled with a third-order MFC, first and second-order being singular on most trajectories.

Contributions

This work develops a third-order Model-Free Controller for a float system equipped with a ballast and a depth sensor. The contributions of this work are the following :

- Design of the first occurrence of a third-order Model-Free Controller applied to a physical system.
- Experimental validation of the third-order MFC on the float with ballast.

As it is the first study of this method on this type of systems, the controller has not yet been compared with other, more conventional or adaptive control methods.

Outline

The paper is organized as follows: Section 2 presents preliminaries to this work, notably a short recap on MFC, the float system, and a quick study of its model. Section 3 exposes the main contribution of this work: the development of the third-order Model-Free Controller and why third order is mandatory. Next, Section 4 presents the experimental results; three different experiments have been conducted: response to a mass disturbance in constant depth regulation, tracking of a trajectory with discontinuous slopes, and tracking of sinusoidal depth reference. The last Section 5 concludes the paper and opens perspectives.

2 Preliminaries

This section presents preliminaries to the contributions of this work. Notably, a short recap on MFC is proposed, as well as a description of the system used in the experiments and a quick study of a coarse dynamic model useful for analysis and tuning of the controller.

2.1 Recap on Model-Free Control

This rapid review on MFC relies on the original work on MFC [11, 12]. Yet, keep in mind that MFC as a control technique is still relatively recent and, to the

authors' best knowledge, has never been applied in the marine context. Slight deviations with the original references thus appear as the authors of this work continuously develop the method.

MFC relies on a rough approximation of the system model, the so-called Ultra-Local Model (ULM) or Homeostat in more recent works [15], which is valid over a short lapse, say $[t-T,t]$ with a "relatively small" $T>0$:

$$y^{(\nu)} = \alpha u + F \tag{1}$$

where the derivation order $\nu \in \mathbb{N}^*$ and the coefficient $\alpha \in \mathbb{R}^*$ are design parameters and F is a time-varying quantity that captures disturbances and mismatches between the unknown physical model and the ULM.[1] This quantity is updated online with estimation techniques stemming from ALIEN estimators [16, 17]. Most MFC applications so far are developed on first-order ULM, and in some cases with a second-order one (see e.g. [18]). Higher order terms are considered disturbances, included in F.

The float with ballast, on the other hand, seems to be the first example where the use of a third-order ULM is mandatory (see section 3.1 for details). Notice that an approximate knowledge of the model can give clues to choose ν [11].

The closed-loop control is constructed on (1) to compensate F by an accurate real-time estimation and a stabilizing term. It is given by:

$$u = \frac{y^{\star(\nu)} + \Lambda_\nu(e) - \widetilde{F}}{\alpha} \tag{2}$$

where Λ_ν is either an *intelligent Proportional controller* (iP) when $\nu = 1$ or an *intelligent Proportional Derivative controller* (iPD) in the case $\nu = 2$ (See Sec. 3.1 below for the case $\nu = 3$.); $e = y^* - y$ is the tracking error and, $\widetilde{F}$ is a real-time estimation of F.

As shown in section 3.2, the algebraic filter used for the estimation of F also acts as a low-pass filter and naturally eliminates noise in the disturbance estimation. This behavior enhances the overall robustness of the method w.r.t noisy measurements.

Note also that is has been demonstrated that the structure of the ALIEN estimator naturally includes the equivalent to the integrator term of a PID controller [19].

2.2 Experimental setup description

The float is depicted on Fig. 1. It is composed of a *BlueRobotics* 100 mm radius watertight cylindrical enclosure containing two *Arduino* microcontrollers. One is dedicated to controlling the ballast and sensor, while the other is devoted to controller calculations.

[1] For example in the present experimentation neither the mass nor the friction coefficient need to be precisely known.

The float is equipped with a single *Alexander Engel KG* ballast system with a 6 V DC motor and a gearbox. A Hall effect sensor has been added to the ballast for precise control of the output water flow rate.

Finally, the system embeds a single *BlueRobotics* Bar02 pressure sensor for depth measurement. This sensor has an estimated measure precision of about 1 cm. To keep the system as minimalistic as possible, there are no additional sensor. The speed and acceleration of the system are obtained with successive differentiation and filtering of the pressure sensor signal. This method introduces bias and noise in critical measurements that will need to be compensated by the controller.

The system can also be equipped with fixed or passively mobile wings as depicted on Fig. 2 and glide while diving and raising. With the wings, the float behaves like a small-scale glider vehicle. This feature motivates the tests presented in the following, and notably the tracking of the sine trajectories, as this trajectory will be used as a guidance principle for surge motion control of the craft.

2.3 Dynamic model of the system

Even though a model-free controller is used to stabilize the system in this work, the study of an approximate system model provides useful information. The float is considered as a single solid exposed to three forces along the vertical axis: its weight, buoyancy, and viscous damping. Note that added mass effects are neglected, and a simple damping scheme is chosen in this work. Newton's second law yields:

$$\ddot{z} = \frac{1}{m_0 + m_b}\left((m_0 + m_b)g - \rho V g - C_f \dot{z}|\dot{z}|\right) \tag{3a}$$

where z is the depth of the float, m_0 is the mass of the system with an empty ballast, m_b is the mass of water contained in the ballast, V is the volume of the enclosure, g is the acceleration of gravity, ρ is the density of water and $C_f > 0$ is a damping coefficient. The volume V and the perceived water density ρ are considered constant and known. The input of the system is the volumetric flow rate of the ballast, denoted u. The relation between u and m_b is:

$$\dot{m}_b = \rho u \tag{3b}$$

which completes the model of the float. Numerical values of the model parameters are given in Table 1.

The relative degree of the output z is three, Eq. (3a) must be differentiated three times for the input u to appear:

$$z^{(3)} = \frac{u\rho(g - \ddot{z}) - 2C_f \ddot{z}|\dot{z}|}{m_0 + m_b} \tag{4}$$

3 Main Contribution: Design of the Model-Free Controller

This section describes the main contribution of this work: the design of the Model-Free Controller used on the float with ballast. The controller differs from the usual MFCs in the literature as it must be of the third order. The novelty notably lies in the structure of Eq. (4) which imposes the use of a third-order ULM. This differs from the original claims of MFC but appears necessary due to the shape of the model as shown in Section 3.1. Moreover, the associated ALIEN estimator [16, 17] and integration procedure are introduced and adapted to this novel constraint, and the complete controller is presented.

3.1 Third Order Ultra-Local Model

The elimination of $(m_0 + m_b)$ between (3a) and (4) leads to:

$$\begin{aligned} & z^{(3)} \left(\rho V g + C_f \dot{z}|\dot{z}|\right) \\ - & (g - \ddot{z}) \left(\rho(g - \ddot{z})u - 2C_f \ddot{z}|\dot{z}|\right) = 0 \end{aligned} \tag{5}$$

which is an input/output relation of the form $E(u, z, \dot{z}, \ddot{z}, z^{(3)}) = 0$.

The calculations of partial derivatives of E w.r.t $z^{(k)}$, $k = 1, 2, 3$ give:[2]

$$\frac{\partial E}{\partial \dot{z}} = 2C_f \left[|\dot{z}| z^{(3)} + (g - \ddot{z}) \operatorname{sign}(\dot{z}) \ddot{z}\right] \tag{6a}$$

$$\frac{\partial E}{\partial \ddot{z}} = 2\left[\rho u(g - \ddot{z}) + C_f |\dot{z}|(g - 2\ddot{z})\right] \tag{6b}$$

$$\frac{\partial E}{\partial z^{(3)}} = \rho V g + C_f |\dot{z}| \dot{z} \tag{6c}$$

where sign stands for the signum function.

Note that $\frac{\partial E}{\partial \dot{z}}$ and $\frac{\partial E}{\partial \ddot{z}}$ are equal to 0 on any constant depth equilibrium of the float and they remain quite small, especially on rest-to-rest slow trajectories (i.e. $\dot{z}$ and $\ddot{z}$ remain small). This implies that the choices $\nu = 1$ and $\nu = 2$ are not viable for the ultra-local model (1) as they would certainly lead to singularities of the control loop. On the contrary, $\frac{\partial E}{\partial z^{(3)}} = \rho V g > 0$ on any rest depth, and $\frac{\partial E}{\partial z^{(3)}} \simeq \rho V g$ on any rest-to-rest slow trajectories. Consequently, the choice $\nu = 3$ appears mandatory to develop the controller. The ultra-local model in the present case is thus:

$$z^{(3)} = \alpha u + F \tag{7}$$

This is, to the authors' best knowledge, the first case for which $\nu > 2$ is mandatory.

Remark 1 *Note that, in this work, the α parameter is taken constant. The recent work of [15] proposes a variable α and a combination of model-based*

[2] See [11, Appendix B] for details.

(flatness) and model-free control but, considering $\frac{\partial E}{\partial z^{(3)}}$ *is quasi constant on slow speed and rest-to-rest trajectories, a variable* α *does not seem to be necessary in a first approach to the method in this quite simple case.*

3.2 Third Order Estimator

The estimate $\widetilde{F}$ of F is built with operational calculus. Assuming $\widetilde{F}$ to be constant on the short time interval $[t-T, t]$, standard techniques of operational calculus, as considered in the ALIEN estimators [16, 17], give:

$$\widetilde{F}(t) = -\frac{7!}{6T^7}\int_0^T \Big[\left[(T-\sigma)^3 - 9(T-\sigma)^2\sigma + 9(T-\sigma)\sigma^2 - \sigma^3\right] y(t-T+\sigma) + \frac{\alpha}{6}\left((T-\sigma)^3\sigma^3\right) u(t-T+\sigma)\Big] d\sigma \tag{8}$$

Note that the size of the time window T is also a tuning parameter of the control law. The integral in (8) acts as a low-pass filter which filters the noise on the measured output y. A larger time window width T improves noise filtering but at the risk of introducing time delays in the closed-loop system. In the following experiments, T has been empirically chosen considering a rough estimate of the time constants of the float. As of today, there is no general method to choose the size of the time window optimally.

In practice, the integral in (8) is discretized with a numerical method and computed in real-time at each sample time. The most popular methods of integration are the Newtown-Cotes formulas [20]. Their expressions rely on a polynomial approximation of the function that has to be integrated. The method's precision increases with the degree of the approximation polynomial, giving each degree a different formula. Note that the functions $(T-\sigma)^3 - 9(T-\sigma)^2\sigma + 9(T-\sigma)\sigma^2 - \sigma^3$ and $(T-\sigma)^3\sigma^3$ in (8) do not depend on time. Consequently, the discrete approximation of the integral relies on coefficients that can be calculated once for all. The calculation corresponding to (8) are simple scalar products between vectors of coefficients and vectors of samples of the measured output and samples of past controls. The global calculation burden is thus light.

Preliminary simulations and corresponding experiments have shown that numerical integration has a considerable impact on the performance of the controller. This has already been pointed out in [21]. Both a *trapezium rule* (degree 1) and a *simple Simpson's rule* (degree 2) lead to steady state error on any equilibrium of the float (rest position at constant depth). Consequently, the *second Simpson's rule*, also named "*Simpson 3/8 method*", which uses a degree 3 approximation polynomial, has been implemented.

3.3 Complete Controller

The controller is calculated in a Feedback Linearization fashion on the ULM (7). The estimate value $\widetilde{F}$ features in the controller and eliminates the need for a conventional integral term even in the presence of disturbances [21, 19]. Because the system is of the third order, an extended iPD regulator featuring

the second time derivative of the tracking error is used to close the loop (details on extended PDs can be found in [22]):

$$u = \frac{1}{\alpha}\left(z^{*(3)} + K_2\ddot{e}_z + K_1\dot{e}_z + K_0 e_z - \widetilde{F}\right) \tag{9}$$

where the K_i's are constant gain parameters, $\widetilde{F}$ is the local estimate of F obtained with (8) and $e_z = z^* - z$ is the error between the reference z^* and the current depth z.

Considering $\widetilde{F} = F$ and applying the controller (9) to the ULM (7) leads to the stable error dynamics:

$$e_z^{(3)} + K_2\ddot{e}_z + K_1\dot{e}_z + K_0 e_z = 0 \tag{10}$$

Note however that Eq. (10) cannot be considered as a formal stability proof since the behavior of the estimator is not studied in this work. The interested reader is referred to [23] for additional study on the stability of MFC. Eq. (10) also gives a hint towards tuning of the gain parameters K_0, K_1 and K_2. Conventional gain tuning methods like pole placement on the simplified closed-loop system give satisfying results and have been used in the experiments of this work.

4 Experimental Results

The main contribution of this work is the experimental validation of the third order MFC on a physical system. This section presents experimental results obtained in the pool at *ENSTA Brest* (see Fig. 3). Three tasks are studied to assess the performance of the controller and its robustness to disturbances and irregularities in the trajectory. First, the system is regulated towards a fixed-depth set point and is manually disturbed with an external mass. Then, the system is tested on a trajectory constituted of a set of slopes with speed discontinuities. Finally, it is evaluated on a smooth trajectory resembling a swimming motion, namely a sine wave. These last two experiments can be thought of as first steps towards a regulated swimming motion of the float system equipped with passive fins. For reference, numerical values of the system parameters are given in Table 1.

All three experiments are also presented in the video provided with this work.

4.1 First test: Constant reference and disturbing mass

This experiment is a set-point regulation with a 1 m depth reference. A disturbing mass is placed on top of the float at 20 s and removed at about 100 s. The addition and removal of the disturbing mass is perceived as a sudden change of mass of the system. Such a phenomenon would happen, for instance, if the system deposits a payload of poorly known mass or picks samples up. It is mandatory to ensure that the controller recovers from such a disturbance.

Fig. 4 displays the depth measured by the float during the first experiment compared to the desired depth. It shows that the system converges towards the fixed reference depth with no overshoot or steady-state error. When the disturbing mass is set on top of the float at 20 s, the system deviates and converges back to the reference in about 40 s. As displayed on Fig. 5, the estimated $\widetilde{F}$ compensates for the disturbing mass and converges back to zero once the float is back on the reference. The same goes when the disturbing mass is removed from the float. This first experiment allows for fine tuning of the control parameters and displays the natural robustness of MFC and Extended iPDs to mass disturbances.

4.2 Second test: Discontinuous slope trajectory

In the second experiment, the system is evaluated on a discontinuous-slope trajectory tracking mission. The task is composed of dives and rises at constant speed. The speed reference has a discontinuity at the change of direction. The goal of this experiment is to assess the performances of the system at constant diving and rising speeds as well as to study its robustness to discontinuities in the reference. On third order systems, step speed references often generate lag errors, where the speed converges towards the step reference but the position moves in parallel to the trajectory. The usual fix to lag errors is the addition of an integral term in the trajectory. This experiment thus validates the integral effect of the estimator function of the extended iPD.

Figs. 6 and 7 respectively display the depth of the float and the tracking error between the float and the reference. The float converges towards the reference with no overshoot, steady-state or lag error during the constant speed dives and rises. At the direction switch, a small overshoot is observed which eventually cancels out. Discontinuous references are notoriously complicated to manage for high order systems. MFC displays good robustness to the discontinuity in this experiment.

On Fig. 7 a first "spike" at zero can be seen at around 10 s before the error increases again. This is likely due to lag error building up and being cancelled out once the estimator $\widehat{F}$ is sufficiently "charged" similarly to the integral term of a conventional PID.

m_0	4.6 kg	T	15 s
V	5×10^{-3} m^3	K_0	0.1
Disturbing mass	50 g	K_1	1.5
α	5×10^3	K_2	2.5

Table 1: System parameters for the float used in the experiments.

4.3 Third experiment: Sinusoidal reference

The third experiment in a more conventional trajectory tracking mission where the reference is a $\mathcal{C}^\infty$ sine function. The parameters of the sine reference function will ultimately become the inputs of the swimming motion of the float equipped with passive fins.

Fig. 9 and Fig. 10 display the depth of the system and the tracking error respectively. The system performs remarkably well in trajectory tracking of the sine reference.

For reference, Fig. 11 displays $\widetilde{F}$ during the third experiment. A sinusoidal signal at the reference frequency can be observed on Fig. 11 with several superimposed high frequency signals. The shape of $\widetilde{F}$ compared to the other two experiments illustrates the compensation of the unmodeled dynamic effects acting on the system on the sine wave trajectory.

5 Conclusion

This work presents an experimental validation of the third-order Model-Free Controller on a minimalistic float equipped with a ballast. This example is the first case to be recorded where a third-order Ultra-Local Model is mandatory. The third-order MFC displays very good performance on the three trajectories tested in this work. The three experiments presented in this work allow demonstrating the robustness of the controller to common disturbances, first to a sudden change of mass, then to lag error due to step speed references on slope trajectories and finally due to unmodeled dynamic effects. The last experiment demonstrates the good performance of the controller on a continuous trajectory tracking application.

The experiments of this work have been conducted only with a depth sensor. The speed and acceleration of the craft are calculated with successive differentiation of the depth measure. Future work will be conducted, adding an Inertial Measurement Unit (IMU) and Complementary Filtering to the system for a more precise acceleration measure.

These results, and notably the tracking of the sine wave reference, will be used as a basis for studies on the swimming motion of the system equipped with passive fins. They also show that the controller is suited for typical marine applications like sample picking, constant depth measures, ...

This work will open up several advanced studies with the float system. First, based on the recent results of the *HEOL* setting [15], more advanced controllers relying on partial knowledge of the model of the vehicle will be developed. The Model-Free Controller will then be compared with other conventional controller, adaptive controllers and controller/estimator associations. Several experiments on the association of Kalman filters and controllers based on estimated models will be conducted and compared to the MFC setting.

References

[1] "Argo." [Online]. Available: https://argo.ucsd.edu

[2] Y. Bai, R. Hu, Y. Bi, C. Liu, Z. Zeng, and L. Lian, "Design and depth control of a buoyancy-driven profiling float," *Sensors*, vol. 22, no. 7, 2022.

[3] S. L. Reste, V. Dutreuil, X. André, V. Thierry, C. Renaut, P.-Y. L. Traon, and G. Maze, "DEEP-ARVOR: A new profiling float to extend the argo observations down to 4000-m depth," *Journal of Atmospheric and Oceanic Technology*, vol. 33, no. 5, pp. 1039–1055, 2016.

[4] B. McGilvray and C. Roman, "Control system performance and efficiency for a mid-depth lagrangian profiling float," in *IEEE OCEANS'10*, Sydney, Australia, 2010, pp. 1–10.

[5] T. Le Mézo, G. Le Maillot, T. Ropert, L. Jaulin, A. Ponte, and B. Zerr, "Design and control of a low-cost autonomous profiling float," *Mechanics & Industry*, vol. 21, no. 512, 2020.

[6] T. Harrison, A. Ziemann, J. Noe, B. Shappell, and K. Morgansen, "Evaluation of two depth-holding algorithms for a buoyancy-controlled coastal float," in *IEEE OCEANS'22*, Hampton Roads, VA, 2022, pp. 1–9.

[7] H. Zhou, J. Fu, Z. Zeng, C. Yu, Z. Wei, B. Yao, and L. Lian, "Adaptive robust tracking control for underwater gliders with uncertainty and time-varying input delay," *Ocean Engineering*, vol. 240, p. 109945, 2021.

[8] W. M. Bessa, E. Kreuzer, J. Lange, M.-A. Pick, and E. Solowjow, "Design and adaptive depth control of a micro diving agent," *IEEE Robotics and Automation Letters*, vol. 2, no. 4, pp. 1871–1877, 2017.

[9] F. Zhang, J. Hou, D. Ning, and Y. Gong, "Depth control of an oil bladder type deep-sea auv based on fuzzy adaptive linear active disturbance rejection control," *Machines*, vol. 10, no. 3, 2022.

[10] M. Fliess, C. Join, M. Mboup, and H. Sira-Ramírez, "Vers une commande multivariable sans modèle," in *IEEE Conférence internationale francophone d'automatique, CIFA'06*, Bordeaux, France, 2006.

[11] M. Fliess and C. Join, "Model-free control," *Int. J. Contr.*, vol. 86, no. 12, pp. 2228–2252, 2013.

[12] ——, "An alternative to proportional-integral and proportional-integral-derivative regulators: Intelligent proportional-derivative regulators," *Int. J. Robust Nonlin. Contr.*, vol. 32, pp. 9512–9524, 2021.

[13] J. M. Barth, J.-P. Condomines, M. Bronz, J.-M. Moschetta, C. Join, and M. Fliess, "Model-free control algorithms for micro air vehicles with transitioning flight capabilities," vol. 12, p. 175682932091426.

[14] Z. Bingul and K. Gul, "Intelligent-PID with PD feedforward trajectory tracking control of an autonomous underwater vehicle," *Machines*, vol. 11, no. 2, p. 300.

[15] C. Join, E. Delaleau, and M. Fliess, "Flatness-based control revisited: The HEOL setting," *Comptes rendus mathématique*, 2024, (to appear, preprint available on `https://arxiv.org/pdf/2408.11580`).

[16] M. Fliess and H. Sira-Ramírez, "An algebraic framework for linear identification," *ESAIM Contr. Optimiz. Calcul. Variat.*, vol. 9, pp. 151–168, 2003.

[17] M. Mboup, C. Join, and M. Fliess, "Numerical differentiation with annihilators in noisy environment," *Numerical Algorithms*, vol. 50, no. 4, pp. 439–467, 2009.

[18] M. Bekcheva, C. Join, and H. Mounier, "Cascaded model-free control for trajectory tracking of quadrotors," in *International Conference on Unmanned Aircraft Systems, ICUAS'18*, Dallas, TX, Jun 2018.

[19] B. d'Andrea Novel, M. Fliess, C. Join, H. Mounier, and B. Steux, "A mathematical explanation via "intelligent" PID controllers of the strange ubiquity of PIDs," in *IEEE 18th Mediterranean Conference on Control and Automation, MED'10*, 2010, pp. 395–400.

[20] K. E. Atkinson, *An Introduction to Numerical Analysis*, 2nd ed. John Wiley & Sons, 1989.

[21] P. Polack, S. Delprat, and B. d'Andréa Novel, "Brake and velocity model-free control on an actual vehicle," *Control Engineering Practice*, vol. 92, no. 104072, pp. 151–168, 2019.

[22] V. Hagenmeyer and E. Delaleau, "Exact feedforward linearization based on differential flatness," *International Journal of Control*, vol. 76, no. 6, pp. 537–556, 2003.

[23] E. Delaleau, "A proof of stability of model-free control," in *Proc. IEEE Conference on Norbert Wiener in the 21st Century (21CW)*, Boston, MA, 2014, pp. 1–7.

Figure 1: The float system. On the top cap, clockwise: Pressure valve, Water inlet, LED, ON/Off button, Bar02 Pressure sensor

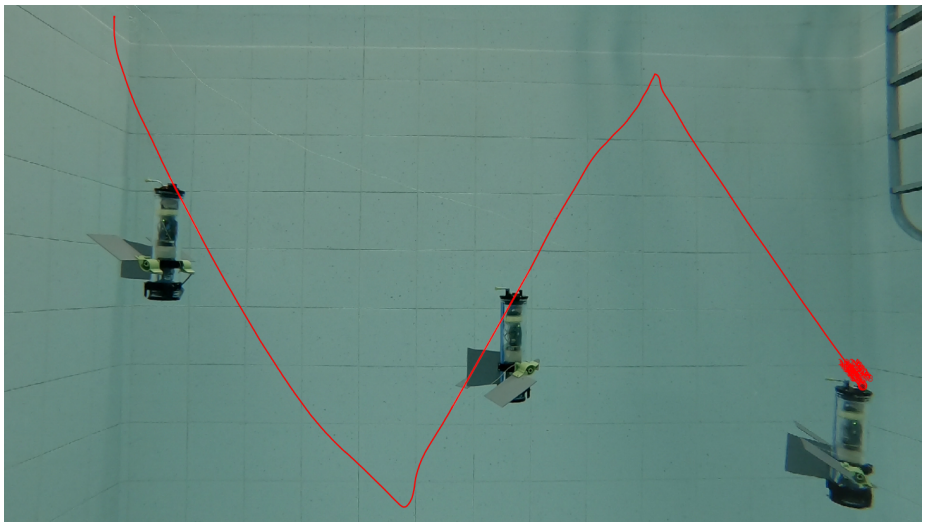

Figure 2: The float equipped with passive mobile wings on a slope-trajectory tracking mission. Three photos of the float are superimposed to show its forward movement. The red line represents the trajectory of the float in the (x_0, z_0) plane

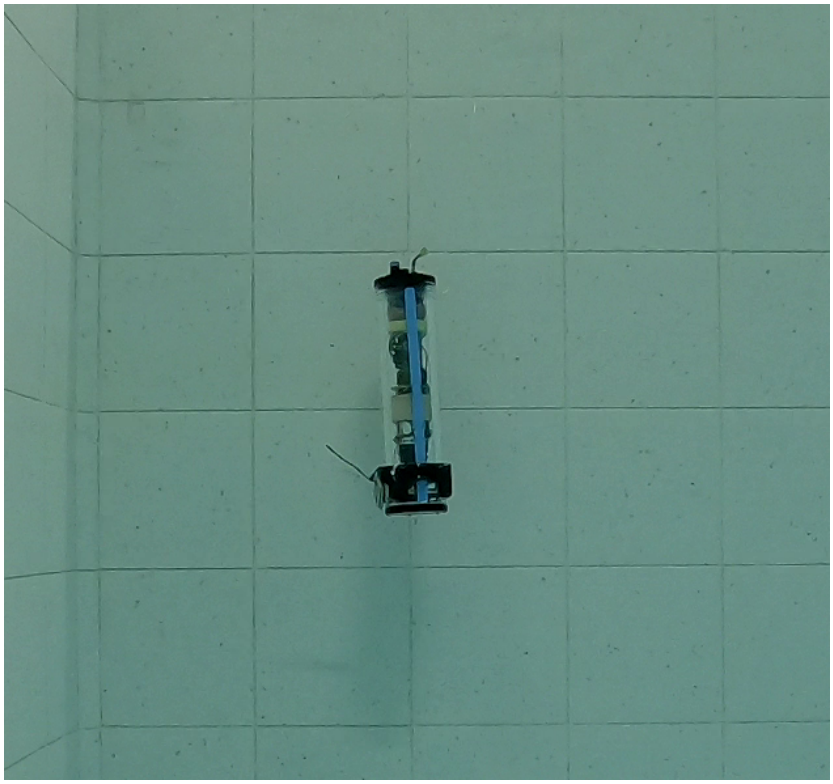

Figure 3: The float with ballast without wings during the experiments in the *ENSTA Brest* test pool.

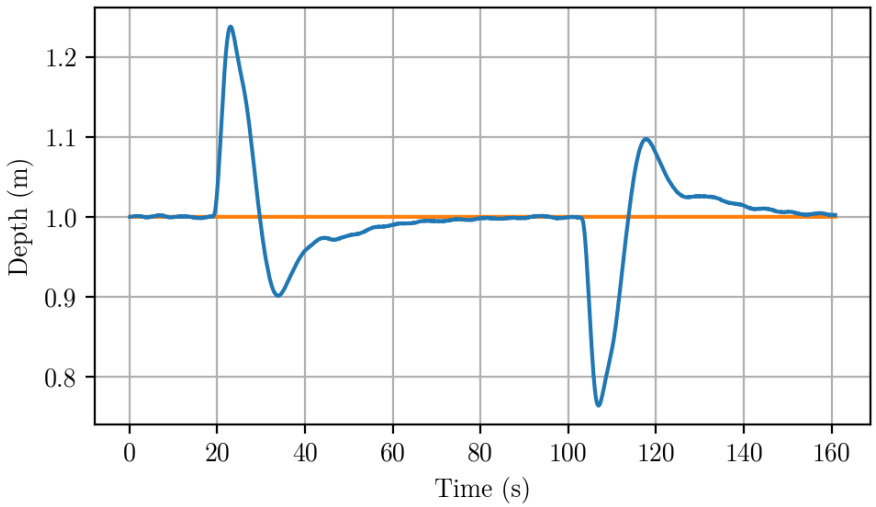

Figure 4: Depth on the set-point regulation with disturbing mass. Blue: Measured depth, Orange: Reference

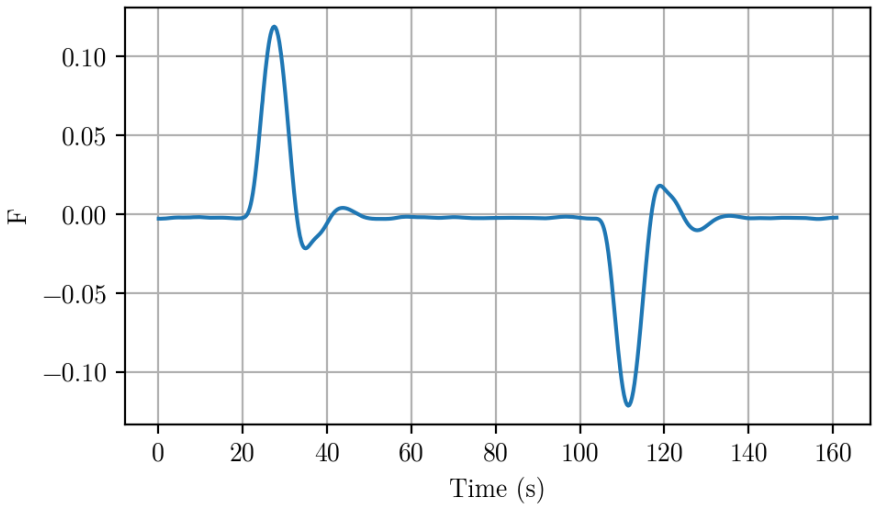

Figure 5: Estimated $\widetilde{F}$ during the set-point regulation with disturbing mass.

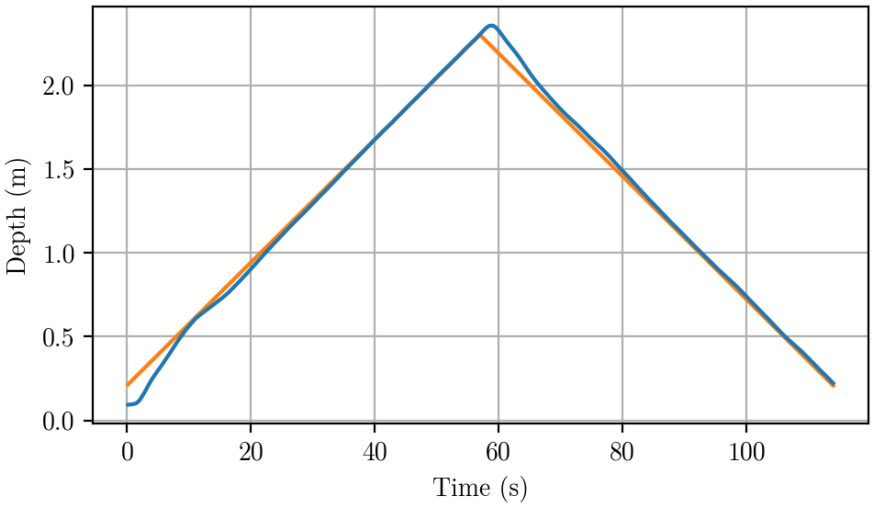

Figure 6: Depth on the successive slopes trajectory. Blue: Measured depth, Orange: Reference

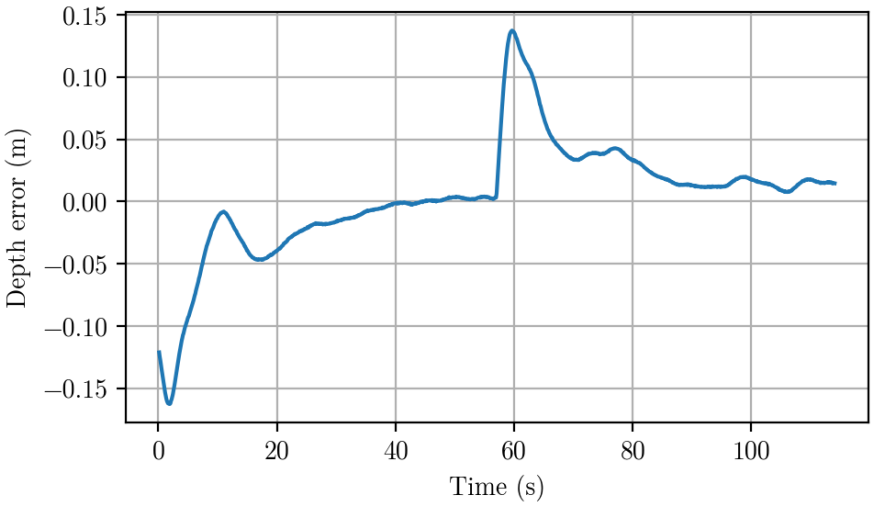

Figure 7: Tracking error on the successive slopes.

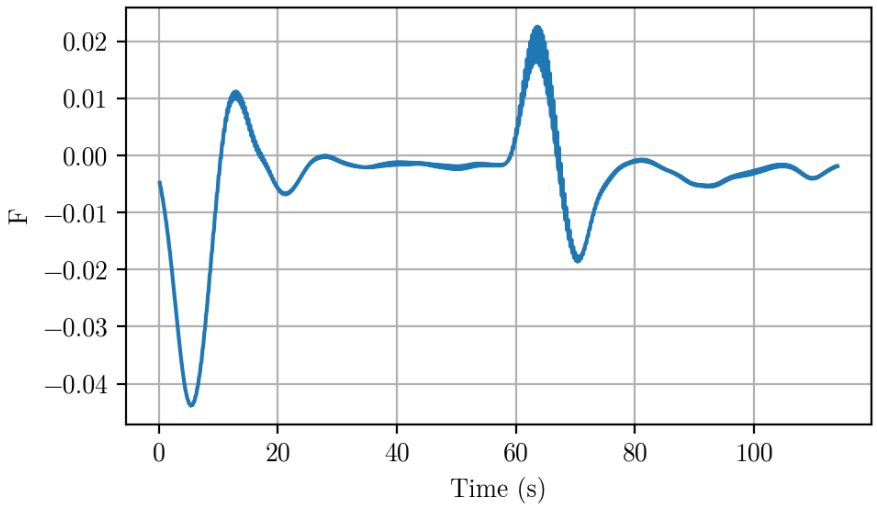

Figure 8: Estimated $\widetilde{F}$ on the successive slopes.

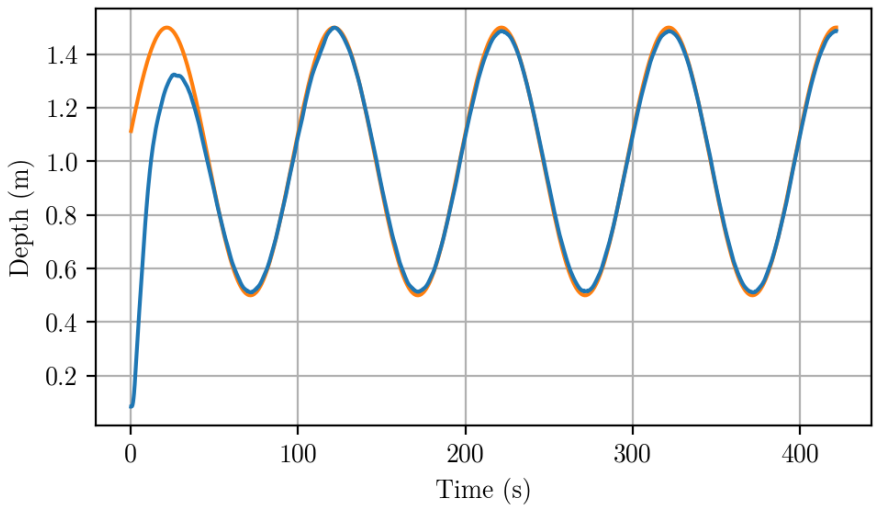

Figure 9: Depth on the sinusoidal trajectory. Blue: Measured depth, Orange: Reference

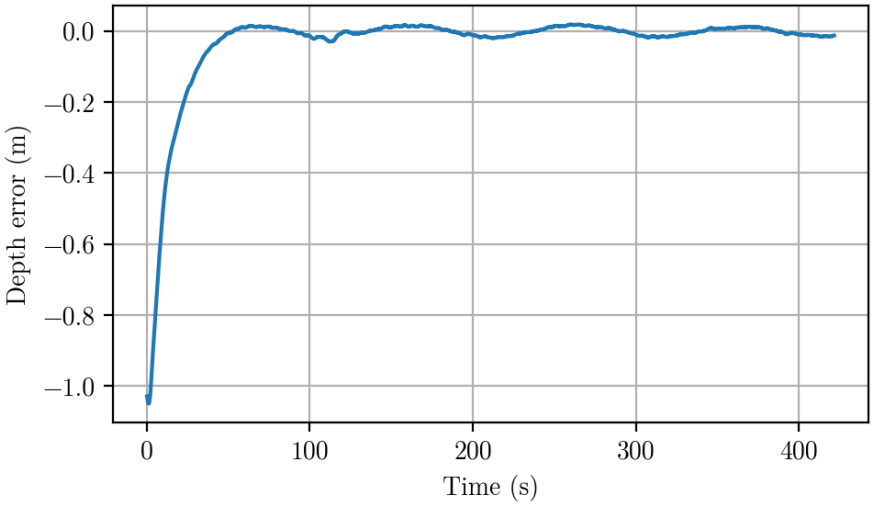

Figure 10: Tracking error on the sinusoidal trajectory.

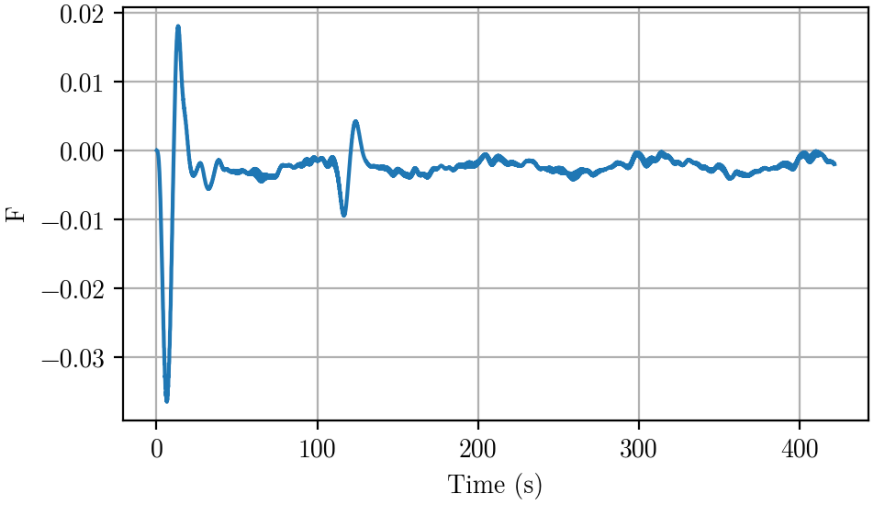

Figure 11: Estimated $\widetilde{F}$ on the sinusoidal trajectory.